Characteristic Analysis and Electrical Conductivity of Graphene and Graphene-Nanosilver Prepared by Electrical Spark Discharge Method

Kuo-Hsiung Tseng (khtseng@ee.ntut.edu.tw)
National Taipei University of Technology
Chu-Ti Yeh
National Taipei University of Technology
Hsueh-Chien Ku
National Taipei University of Technology
Der-Chi Tien
National Taipei University of Technology
Leszek Stobinski
Warsaw University of Technology

Research Article

Keywords: Electrical spark discharge method, Graphene, Graphene-Ag, Conductivity

Posted Date: September 23rd, 2021

DOI: https://doi.org/10.21203/rs.3.rs-919197/v1

Characteristic Analysis and Electrical Conductivity of Graphene and Graphene-Nanosilver Prepared by Electrical Spark Discharge Method

Kuo-Hsiung Tseng[a,*], Chu-Ti Yeh[a], Hsueh-Chien Ku[a], Der-Chi Tien[a], and Leszek Stobinski[b]
[a]Department of Electrical Engineering, National Taipei University of Technology, Taipei 10608, Taiwan, R.O.C.
[b]Materials Chemistry, Warsaw University of Technology, Warynskiego 1, 00-645 Warsaw, Poland
*Correspondence should be addressed to Kuo-Hsiung Tseng: khtseng@ee.ntut.edu.tw

ABSTRACT
This study used an electric discharge machine (EDM) to perform the electrical spark discharge method (ESDM) to prepare a graphene colloid and a graphene-Ag colloid. The characteristic wavelengths of graphene, and graphene-Ag are both 262 nm. They had the properties of high dispersion and are unlikely to aggregate. The XRD patterns of graphene and graphene-Ag are typical carbon diffraction peak angles and crystal orientations. Graphene-Ag in DW can increase the Raman signal intensity of graphene. Regarding the graphene colloid and graphene-Ag colloid, their average sheet resistance values are 0.0329 MΩ/sq and 0.00136 MΩ/sq, respectively. Moreover, when AgNPs composited with graphene layers, the average sheet resistance is only 1/24 that of graphene layers, indicating that graphene-Ag has superior conductivity.
Keywords: Electrical spark discharge method, Graphene, Graphene-Ag, Conductivity

1. Introduction

Graphene consists of a single layer of graphite. Its structure is a two-dimensional thin film honeycomb lattice formed with carbon atoms in an sp^2 hybrid orbital [1]. The thickness of graphene is only one carbon atom. The thickness of perfect one-layer graphene is 0.34 nm [2]. The distance of the C–C bond is 0.14 nm, which is the thinnest among all existing materials. It is a structurally stable and tough two-dimensional material. The potential applications of graphene, including integrated circuits (ICs)[3-4], super capacitors[5-6], transparent conductive electrodes[7-8], dye-sensitized solar cells[9-10], thermal conductive materials[11-12], and antibacterial applications[13-14].Graphene is a type of semimetal or zero-band-gap semiconductor. At room temperature, when electron transport is measured, the results indicate that graphene exhibits high electron mobility, with a mobility rate of approximately 200,000 $cm^2 \cdot V^{-1} \cdot s^{-1}$. The resistivity that corresponds to this value is 10^{-8} Ω·m, whereas the resistivity of silver is 10^{-8} Ω·m. Because the resistivity of graphene is slightly lower than silver, this means that it has superior conductivity to silver, making it the material with the highest conductivity in existence [15].

EDM is an unconventional machining method. It utilizes the ESDM to process conductive materials. The principle is to convert electricity into heat and use high energy to cut conductive materials[16-17]. First, a conductive material is placed between the upper electrode (the item that conducts processing) and the lower electrode (the item to be processed) and is soaked in a dielectric fluid with high insulation performance [18]. The dielectric fluid can be DW or an insulating liquid. DC pulse voltage is applied between the two electrodes to form an electric field. Subsequently, the servo control system pushes the upper electrode slowly toward the lower electrode. The discharge state and distance between the two electrodes are critical factors affecting the machining quality. The heat generated by the electric arc increases the temperature of the electrode surface up to 6000–10,000°C. The high temperature causes the electrodes to melt and vaporize. Simultaneously, minute particles peel from their surface. These particles rapidly cool, condense, and spread in the dielectric fluid. At this moment, the discharge pulse stops. The surfaces of the two electrodes return to being insulated, awaiting the discharge pulse of the next cycle. Through the aforementioned method, using periodic discharge,

conductive materials can be processed [19].

2. Experimental system and method

2.1. Experimental system

Figure 1 is a composition schematic of an EDM. When creating nanocolloids, the conductive materials prepared in advance are loaded onto the electrodes, and the lower electrode is connected to a DC power negative. Corresponding parameters values are set on the control panel to output different levels of discharge pulse, current, power, and stability. When the two electrodes are emerged in the dielectric fluid to initiate discharge processing, electrons in the dielectric fluid move from the negative electrode to positive electrode. The amount of metal consumed at the lower electrode is greater than that at the upper electrode; thus, the lower electrode is called the processed end, whereas the upper electrode is called the processing end. To ensure that tip of the electrode surface discharges stably, the lower and upper electrodes are usually made of conductive materials with a wire diameter of 2 mm and 1 mm, respectively. The two electrodes are placed in a dielectric fluid for the ESDM. The prepared nanocolloids are stored in scintillation counting vials. To prevent the carbon depositing of the two electrodes during the preparation process, which would cause a short circuit, a magnetic stirrer is placed underneath the storage container. The magnetic stirrer rotates the stir bar in the storage container so that the generated nanoparticles distribute in the dielectric fluid evenly. Before the discharge procedure begins, the upper and lower electrodes must be aligned. This can be done through adjusting the cross slide by rotating the bidirectional wheel axle. Finally, the control panel is used to set parameters, and the servo control system is used to control the distance between the two electrodes. An extremely small distance can effectively form spark discharge, enabling a smooth discharge process.

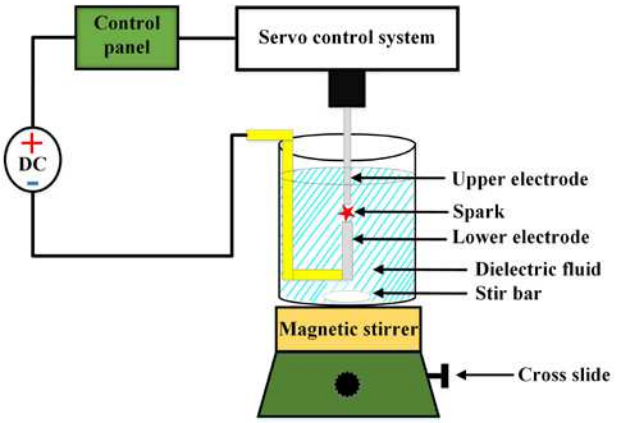

Figure 1. Schematic of EDM

EDM is a discharge process that involves the generation of sparks [20]. Two electrodes are kept in the dielectric fluid in an insulating state before being provided with a DC pulse power source. This forms a current channel between the two electrodes, destroying the insulating state of the dielectric fluid and generating sparks. Next, the electric energy is converted to heat energy, and the high temperature generated by the heat energy melts the surface of the material of the electrode. The material on the surface peels off, cools, and forms nanoparticles. Finally, the particles disperse in the dielectric fluid, which returns to the insulating state. The EDM discharge process is illustrated in Figure 2 and explained below.

(a) Preparation for discharge: The upper and lower electrodes of the electrode materials are soaked in the dielectric fluid. The two ends of the electrodes are connected to a DC power source and are confirmed to be aiming directly at each other. In this state, there is no voltage or current, and the dielectric fluid is in an insulating state.

(b) Discharge initiation: When the discharge cycle begins, T_{on} begins and V_{gap} increases. When the upper electrode slowly moves toward the lower electrode until the distance between the two are extremely small, the electric field strength at the gap between the two electrodes exceeds the dielectric strength of the dielectric fluid. Electrons are injected from the surface of the lower electrode into the upper electrode. Molecules in the dielectric fluid become ionized, and the gap between the electrodes gradually establishes a discharge channel.

(c) Ionization: When the insulating state in the gap between the two electrodes is destroyed, electrons depart from the lower electrode, impact the neutral atoms in the dielectric fluid between the electrodes, and excite valence electrons at the most outer layer of the atoms to form positive ions and free electrons. At this time, electrons rapidly flow to the upper electrode, conduct ionization again, and form an ionization channel. I_{gap} increases and V_{gap} decreases.

(d) Melting: When discharge succeeds, Igap is maintained at its maximum value. The positive ions and free electrons keep impacting the upper and lower electrodes. When they impact the surface of the electrodes, the kinetic energy instantly turns into heat, forming a discharge spark. This high heat melts and evaporates the surface of the electrodes, and the metal electrode surface peels off nanoparticles.

(e) End of discharge: T_{off} begins, and V_{gap} and I_{gap} decrease. When the pulse voltage and pulse current enter the T_{off} state, electrodes stop releasing electrons and the current starts to reduce. The ionized channel rapidly disappears. The nanoparticles that melted and peeled off from the electrode surface are suspended in the dielectric fluid. The gap voltage and gap current reduce.

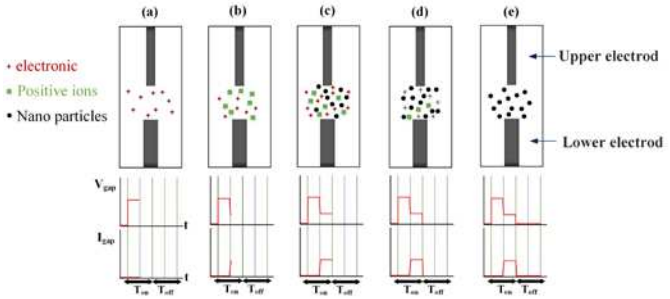

Figure 2. The EDM discharge process: (a) preparation for discharge, (b) discharge initiation, (c) ionization, (d) melting, (e) end of discharge

2.2 Dielectric fluid and material

The dielectric fluid used are DW. The graphite electrode materials are presented in Figure 3. The upper and lower electrodes both used graphite rods, which were made from entire graphite of 99.9% purity; through lathe processing, the graphite was burned into a chunk with features and size suitable for discharge processing. Graphite-silver electrode materials are illustrated in Figure 4. Entire graphite of 99.9% purity was used. During processing, silver was added to burn into a chunk to generate a graphite-silver rod with features and size suitable for discharge processing.

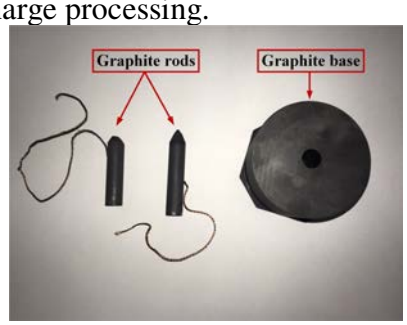

Figure 3. Graphite rod electrodes

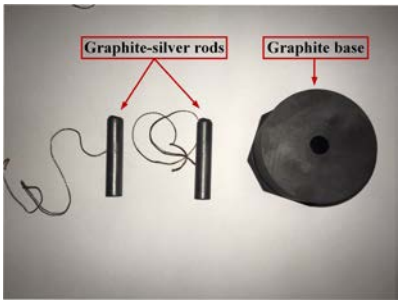

Figure 4. Graphite-silver rod electrodes

2.3 Experimental Method

This study used EDM to prepare a graphene colloid and a graphene-Ag colloid. The environmental parameter settings for the preparation are listed in Table 1. The dielectric fluid used was DW and the amount was 150 mL. T_{on}:T_{off} were set at 30:30 μs and the voltage was set at 140 V. The current was set as the second level. The discharge time for the graphene colloid was 27 min. To fix the lower electrode in a container, entire graphite of 99.9% purity was processed into a shape that could be fixed in the base of the lower electrode and then placed in the container. The environmental parameter settings for preparing the graphene-Ag colloid are listed in Table 2. The dielectric fluid used was DW and the amount was 150 mL. T_{on}:T_{off} were set at 30:30 μs and the voltage was set at 140 V. The current was set as the second level. The discharge time was 3.5 min. The proportion of graphite and silver in the graphite-silver rod was 70% and 30%. The upper and lower electrodes of

the EDM were both graphite-silver rods.

Table 1. Environmental Parameter Settings for Preparing Graphene Colloid

Title	Parameter
Electrode	Graphite rod
T_{on}:T_{off}	30:30 μs
Current segment	2
Voltage	140 V
Dielectric fluid	DW
Volume of the dielectric fluid	150 mL
Discharge time	27 min
Temperature	25 ℃
Atmospheric pressure	1 atm

Table 2. Environmental Parameter Settings for Preparing Graphene-Ag Colloid

Title	Parameter
Electrode	Graphite-silver rod
T_{on}:T_{off}	30:30 μs
Current segment	2
Voltage	140 V
Dielectric fluid	DW
Volume of the dielectric fluid	150 mL
Discharge time	3.5 min
Temperature	25 ℃
Atmospheric pressure	1 atm

3. Results and Discussion

3.1 Suspension stability

The Zetasizer is used to analyze the suspension stability of graphene and graphene-Ag. The analysis results are presented as zeta potential. The suspension stability analysis results of graphene is presented in Figure 5(a). The analysis results in Figure 5(a) reveal that the zeta potential of graphene is −34.6 mV. The absolute zeta potential value is greater than 30 mV, indicating that this colloid had favorable suspension stability. The suspension stability analysis results of graphene-Ag is presented in Figure 5(b). Figure 5(b) reveals that the zeta potential of graphene-Ag is −40.6 mV, meaning that this colloid also had favorable suspension stability. Because AgNP had an excellent suspension ability, when AgNPs formed a composite with graphene layers, the suspension stability of graphene-Ag improved. In summmary, the zeta potential of graphene-Ag is greater than that of graphene, demonstrating that graphene-Ag had superior suspension stability to graphene, enabling its wider applicability.

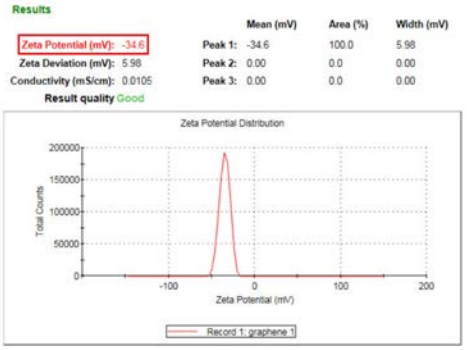

(a)

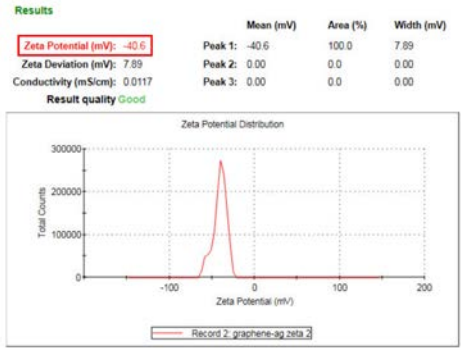

(b)

Figure 5. Zeta potential (a)graphene, (b)graphene-Ag

3.2 Characteristic analysis

UV–Vis is used to analyze the optical properties of graphene and graphene-Ag. The analysis results are presented in Figure 6. The figure shows that graphene had a clear absorption peak that corresponded to the wavelength at 262 nm, and its absorbance is 0.822. This is formed due to sp^2 carbon atoms. This absorbance peak is typical for the UV–Vis spectra of graphene, verifying that graphene can indeed be obtained from EDM. The absorption peaks of graphene-Ag and graphene are very close. The wavelength of the absorption peak of graphene-Ag is also located at 262 nm, which is identical to the characteristic wavelength of graphene, and its absorbance is 0.803. As a result, when the light source of a wolfram lamp passes the sample, it cannot analyze the characteristic wavelength of AgNPs. In summary, we verified that using graphite rods and graphite-silver rods

can prepare graphene and graphene-Ag, respectively, through EDM. The preparation time is short, and no additional chemical agents are required.

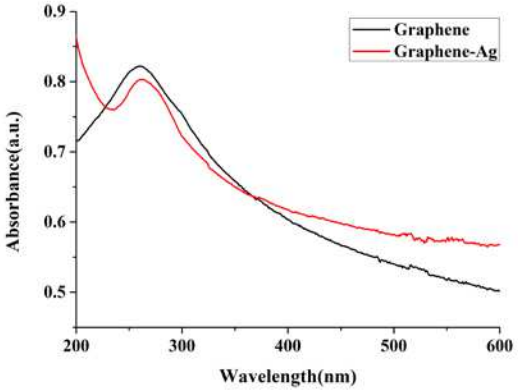

Figure 6. UV–Vis spectra of the graphene and graphene-Ag

XRD is used to analyze the crystal structures of graphene and graphene-Ag. Figure 7 presents the analysis results of the diffraction peak and crystal structure. The figure reveals a diffraction peak of graphene at the position where 2θ is 26.3°. The crystal orientation is (002). From the figure 7, we observed another XRD pattern, which is the graphene-Ag analysis result. The figure 7 shows a clear diffraction peak, whose 2θ (degree) angle is located at 26.4°, and the corresponding crystal orientation is (002). Notably, in the graphene-Ag crystal, a diffraction peak of silver is not observed, meaning that the silver crystal is not detected. In summary, Figure 7 reveals that when using two different types of graphite rods and electrodes, through EDM we are able to prepare carbon-structure colloids with comprehensive crystals with an orientation of (002). Regarding the diffraction peak intensity, because they are two completely different materials and products, the intensities of the two diffraction peaks can be overlooked.

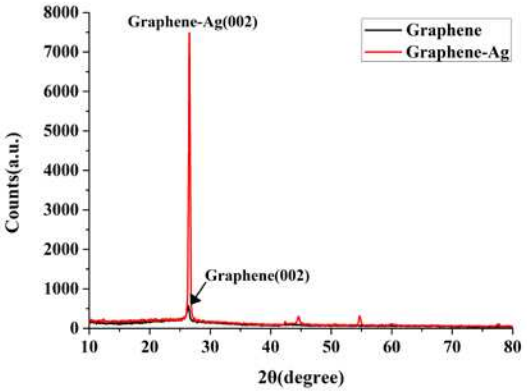

Figure 7. XRD patterns of the graphene and graphene-Ag

Raman is used to analyze the defects and SERS of graphene and graphene-Ag, and the analysis results are presented in Figure 8. The figure shows that the Raman spectra of graphene has two characteristic peaks (D-band and G-band). Their characteristic peaks correspond to the wavenumbers of 1353 cm^{-1} and 1577 cm^{-1}. Using the D-band and G-band intensity ratio, we calculated the intensity ratio of graphene as 0.994 (5910/5944). The Raman spectrum of the graphene-Ag is special in that it has a very small characteristic peak D-band and a very large G-band, meaning that the graphene-Ag is highly graphitized and had few defects. The D-band and G-band corresponded to the wavenumbers of 1353 cm^{-1} and 1575 cm^{-1}, respectively. The intensity ratio of graphene-Ag is 0.854 (10297/12050). According to the intensity ratio, we learned that graphene had more defects compared with graphene-Ag. This is because the electrodes used to prepare graphene-Ag are graphite-silver rods. Silver is a conductor and has favorable conductivity, so its discharge process is smooth and may peel more complete graphene-Ag to be dispersed in DW. From the figure, we could also determine the impact of SERS on graphene and graphene-Ag. The G-band Raman signal intensity of graphene-Ag substantially increased, verifying that using the physical method of the ESDM to prepare graphene-Ag in DW can increase the Raman signal intensity of graphene.

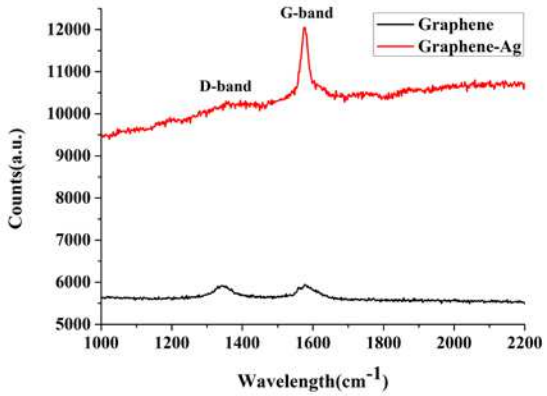

Figure 8. Raman of the graphene and graphene-Ag

TEM is used to analyze the surface properties of graphene and graphene-Ag. Figure 9 presents the TEM image of graphene. Figure 9(a) illustrates clearly the stacking of graphene layers, and we can identify the differences represented by color. The peripheral had less graphene stacked together, so the color is a light gray. Thicker stacks of graphene layers are observed, which exhibited a black color. From the Figure 9 (b), one can see the lattice line of part of the graphene. This lattice line indicates the distance between the graphene layers. In this sample, after measurement, the inter-layer distance is 0.33 nm. Figure 10 presents the TEM image of graphene-Ag. In the Figure 10 (a), numerous round and dark small AgNPs are observed on the graphene layers. The particles are embedded in the graphene layers. The size distribution of AgNPs is presented in Figure 10 (b). This distribution graph is mainly from the AgNP size in the TEM image of Figure 10 (a). The size of small AgNPs is approximately 5 nm; they account for almost half of the AgNPs. This means that when using graphite-silver rods to conduct ESDM processing, we could prepare AgNPs of a very small size embedded in graphene layers.

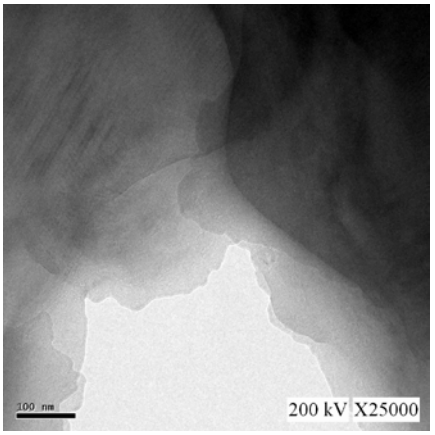

(a)

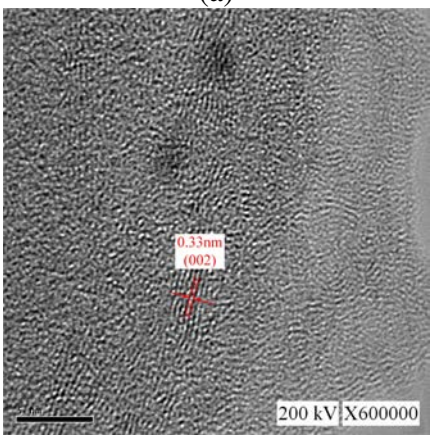

(b)

Figure 9. (a)TEM image of graphene, (b) magnified image of graphene

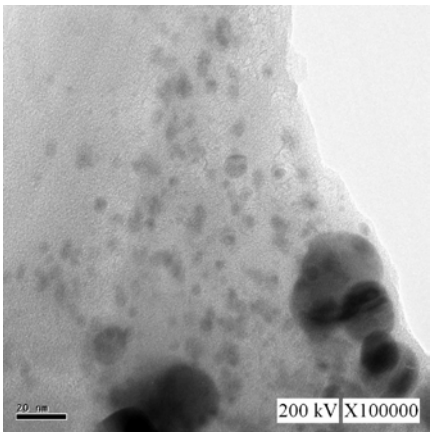

(a)

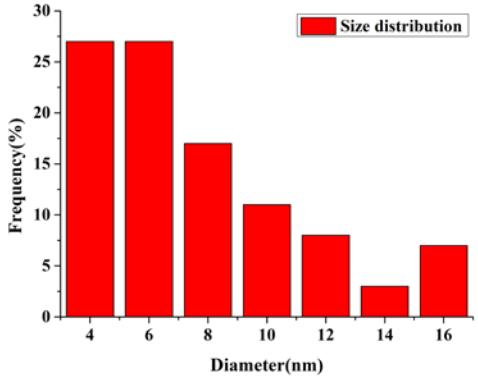

(b)

Figure 10. (a) TEM image of graphene-Ag, (b) particle size distribution of the AgNPs.

3.3 Conductivity

Table 3 lists the conductivity test results of graphene and graphene-Ag. The table lists the sheet resistance of graphene and graphene-Ag measured at 10 different areas on the films. For graphene, the minimum, maximum, and average sheet resistance values are 0.013 MΩ/sq, 0.076 MΩ/sq, and 0.0329 MΩ/sq, respectively. For graphene-Ag, the minimum, maximum, and average sheet resistance values are 0.0006 MΩ/sq, 0.003 MΩ/sq, and 0.00136 MΩ/sq, respectively. The graphene colloid prepared using the ESDM with graphite rods as electrodes is prepared into coating samples. Its average sheet resistance value is 0.0329 MΩ/sq, verifying that under this preparation environment, graphene flakes that peeled in DW are conductive and had favorable dispersion. Regarding the graphene-Ag colloid prepared using graphite-silver as the electrode, its average sheet resistance is 0.00136 MΩ/sq, which is 1/24 that of graphene, indicating that graphene-Ag has superior conductivity and dispersion compared with graphene. In short, we confirmed that using EDM to conduct the ESDM and prepare graphene colloid samples as well as using the coating method to prepare coating samples obtained graphene products with conductivity. In addition, after mixing silver into graphite to prepare the graphene-Ag colloid, when AgNPs and graphene layers became a new composite, the conductivity of graphene-Ag is superior to graphene and rGO-Ag because Ag has excellent conductivity. This substantially increased the possibility of the future application of graphene-Ag to conductive matters, and also met our original goal of not using chemical methods but rather purely using EDM to prepare this composite material.

Table 3. Sheet Resistance Values (MΩ/sq) of Graphene and Graphene-Ag

Area No.	Graphene	Graphene-Ag
1	0.04	0.002
2	0.076	0.002
3	0.029	0.001
4	0.013	0.0006
5	0.03	0.001
6	0.03	0.001
7	0.036	0.001
8	0.02	0.001
9	0.027	0.001
10	0.028	0.003
Average	0.0329	0.00136

4. Conclusions

This study proposed a method for preparing graphene and graphene-Ag by using EDM. The ESDM is a physical preparation method. Compared with chemical synthesis methods, this method is simple, fast, and environmentally friendly. The research results of this dissertation are as follows:

1. The suspension stability test of graphene, and graphene-Ag revealed that the absolute values of their zeta potential are all greater than 30 mV, indicating that the graphene products prepared using the ESDM all had favorable suspension stability. Favorable suspension stability means there is a high mutual repulsion force between graphene layers and nanoparticles. The layers and particles do not aggregate easily, so the colloid can temporarily retain the properties of the nanomaterial, which increases the feasibility of using it in the industry in the future.
2. Through the analysis of surface properties of graphene products, we clearly observed that the shape of graphene is in flakes, and the AgNPs in graphene-Ag are composited on the graphene layers, forming a new type of graphene composite with different properties.
3. Regarding the conductivity analysis, the

average sheet resistance values of graphene, and graphene-Ag are 0.0329 MΩ/sq and 0.00136 MΩ/sq, respectively. The average sheet resistance value of graphene-Ag is only 1/24 that of graphene, indicating that graphene-Ag had a conductivity far superior to that of graphene.

Availability of data and materials

The data used to support the findings of this study are included within the article.

Competing interests

The authors declare that there is no conflict of interest regarding the publication of this paper.

Funding

The Ministry of Science and Technology (MOST 110-2221-E-027-042-).

Acknowledgements

The authors would like to thank the Precision Research and Analysis Center, National Taipei University of Technology for technical supporting this research.

Author Contributions

Project administration, Kuo-Hsiung Tseng; resources, Kuo-Hsiung Tseng; supervision, Kuo-Hsiung Tseng; funding acquisition, Kuo-Hsiung Tseng; data curation, Chu-Ti Yeh and Hsueh-Chien Ku; formal analysis, Chu-Ti Yeh and Hsueh-Chien Ku; methodology, Der-Chi Tien and Leszek Stobinski; validation, Hsueh-Chien Ku and Der-Chi Tien; writing—original draft, Hsueh-Chien Ku; writing—review and editing, Chu-Ti Yeh. All authors have read and agreed to the published version of the manuscript.

References

[1] Wang, J. T., Qian, Y., Weng, H., Wang, E., and Chen, C., "Three-dimensional crystalline modification of graphene in all-sp2 hexagonal lattices with or without topological nodal lines," *The Journal of Physical Chemistry Letters*, vol. 10, no. 10, 2019, pp. 2515-2521.

[2] Sidorov, A. N., Yazdanpanah, M. M., Jalilian, R., Ouseph, P. J., Cohn, R. W., and Sumanasekera, G. U., "Electrostatic deposition of graphene," Nanotechnology, vol. 18, no. 13, 2007, 135301.

[3] Han, S. J., Garcia, A. V., Oida, S., Jenkins, K. A., and Haensch, W., "Graphene radio frequency receiver integrated circuit," Nature communications, vol. 5, no. 1, 2014, pp. 1-6.

[4] Saeed, M., Hamed, A., Wang, Z., Shaygan, M., Neumaier, D., & Negra, R. (2018). Graphene integrated circuits: new prospects towards receiver realisation. Nanoscale, 10(1), 93-99.

[5] Jost, K., Dion, G., and Gogotsi, Y., "Textile energy storage in perspective," Journal of Materials Chemistry A, vol. 2, no. 28, 2014, pp. 10776-10787.

[6] Huang, Y., Liang, J., & Chen, Y. (2012). An overview of the applications of graphene−based materials in supercapacitors. small, 8(12), 1805-1834.

[7] Wang, Y., Chen, X., Zhong, Y., Zhu, F., and Loh, K. P., "Large area, continuous, few-layered graphene as anodes in organic photovoltaic devices," Applied Physics Letters, vol. 95, no. 6, 2009, 209.

[8] Woo, Y. S. (2019). Transparent conductive electrodes based on graphene-related materials. Micromachines, 10(1), 13.

[9] Longo, C., and De Paoli, M. A., "Dye-sensitized solar cells: a successful combination of materials," Journal of the Brazilian Chemical Society, vol. 14, no. 6, 2003, pp. 898-901.

[10] Roy-Mayhew, J. D., & Aksay, I. A. (2014). Graphene materials and their use in dye-sensitized solar cells. Chemical reviews, 114(12), 6323-6348.

[11] Matsumoto, T., Koizumi, T., Kawakami, Y., Okamoto, K., and Tomita, M., "Perfect blackbody radiation from a graphene nanostructure with application to high-temperature spectral emissivity measurements," Optics express, vol. 21, no. 25, 2013, pp. 30964-30974.

[12] Shahil, K. M., & Balandin, A. A. (2012). Thermal properties of graphene and

multilayer graphene: Applications in thermal interface materials. Solid state communications, 152(15), 1331-1340.
[13] Ji, H., Sun, H., and Qu, X., "Antibacterial applications of graphene-based nanomaterials: recent achievements and challenges," Advanced drug delivery reviews, vol. 105, 2016, pp. 176-189.
[14] Ma, J., Zhang, J., Xiong, Z., Yong, Y., and Zhao, X. S., "Preparation, characterization and antibacterial properties of silver-modified graphene oxide," Journal of Materials Chemistry, vol. 21, no. 10, 2011, pp. 3350-3352.
[15] Balandin, A. A., Ghosh, S., Bao, W., Calizo, I., Teweldebrhan, D., Miao, F., and Lau, C. N., "Superior thermal conductivity of single-layer graphene," Nano letters, vol. 8, no. 3, 2008, pp. 902-907.
[16] Tseng, K. H., Ku, H. C., Tien, D. C., and Stobinski, L., "Novel preparation of reduced graphene oxide–silver complex using an electrical spark discharge method," Nanomaterials, vol. 9, no. 7, 2019, 979.
[17] Tseng, K. H., Chang, C. Y., Chung, M. Y., & Cheng, T. S., "Fabricating TiO2 nanocolloids by electric spark discharge method at normal temperature and pressure." Nanotechnology, vol. 28, no. 46, 2017, 465701.
[18] Hockenberry., T. O., "The Role of the Dielectric Fluid in Electrical Discharge Machining," SAE Technical Paper, 1968.
[19] Tseng, K. H., Ku, H. C., Tien, D. C., and Stobinski, L., "Parameter control and concentration analysis of graphene colloids prepared by electric spark discharge method," Nanotechnology Reviews, vol. 8, no. 1, 2019, pp. 201-209.
[20] Tseng, K. H., Lin, Y. H., Tien, D. C., Ku, H. C., and Stobinski, L., "Stability analysis of platinum nanoparticles prepared by ESDM in deionised water," Micro & Nano Letters, vol. 13, no. 11, 2018, pp. 1545-1549.